IEEE Open Journal of
Industry Applications

Received 26 September 2023; revised 28 February 2024 and 2 April 2024; accepted 7 May 2024. Date of publication 10 May 2024; date of current version 21 May 2024. The review of this article was arranged by Associate Editor Shafiq Odhano.

Digital Object Identifier 10.1109/OJIA.2024.3399603

Bidirectional Hybrid DC Circuit Breaker With Zero Voltage and Current Switching for Radar Power System

NANDAKUMAR SAMINATHAN [1,2] (Member, IEEE), ADITYA P [3] (Graduate Student Member, IEEE), SATISH NAIK BANAVATH [3] (Senior Member, IEEE), ALESSANDRO LIDOZZI [4] (Member, IEEE), MARCO DI BENEDETTO [5] (Member, IEEE), AND A VENGADARAJAN [6] (Senior Member, IEEE)

[1]Department of Electrical, Electronics, and Communication Engineering, Indian Institute of Technology Dharwad, Dharwad 580011, India
[2]Electronics and Radar Development Establishment, Bengaluru 560093, India
[3]Department of Electrical, Electronics, and Communication Engineering, Indian Institute of Technology Dharwad, Dharwad 580011, India
[4]C-PED, Center for Power Electronics and Drives, Roma Tre University, 00146 Roma, Italy
[5]Department of Industrial, Electronic and Mechanical Engineering, Roma Tre University, 00146 Roma, Italy
[6]Electronics and Radar Development Establishment, Bengaluru 560093, India

CORRESPONDING AUTHOR: ALESSANDRO LIDOZZI (e-mail: alessandro.lidozzi@uniroma3.it)

This work was supported by the SERB, Department of Science and Technology (DST), India under Grant EEQ/2023/000017.

ABSTRACT This article proposes a novel zero-voltage switching (ZVS) and zero-current switching (ZCS)-based hybrid dc circuit breaker for a radar power system. Long-range radars demand huge power, in the order of hundreds of kW. Radar's phased array antenna houses a large number of electronic devices and works primarily on a dc power supply. Typically, military systems are required to have the highest operational reliability, as a result, electrical system protection plays a crucial role. A high power 310 V dc electrical power grid in radar carries hundreds of amperes of current under nominal operating conditions, results in significant fault current due to very low impedance, and demands a very fast fault interruption device. This article proposes and demonstrates the complete operation of a hybrid dc circuit breaker topology for radar applications. The proposed dc circuit breaker employs a mechanical switch that carries the entire current during the nominal operating conditions, and a power electronic module (PEM) connected in parallel helps in diverting the fault current from the main path. Fault current transfers to the PEM branch in a fraction of a second (5 μs), which ensures faster load-side isolation. During the fault interruption process, mechanical switch contact opening experiences both ZVS and ZCS features, resulting in arcless operation, and also helps in faster contact separation. The ZVS and ZCS features greatly improve the reliability of the mechanical switch. The proposed concept does not involve any capacitors or corresponding precharging circuits for the ZVS/ZCS features. The proposed dc circuit breaker is analyzed theoretically, and also by simulations in LTspice. Additionally, an experimental prototype with a dc system rating of 310 V–10 A is developed to experimentally validate the performance of the proposed breaker topology. The article also presents a detailed design and comparative analysis, along with a discussion on the limitations of the proposed dc circuit breaker, and the scope for improvements.

INDEX TERMS Current-limiting, high-speed current interruption, hybrid dc circuit breaker, mechanical circuit breaker (MCB), radar power system (RPS), solid-state dc circuit breaker.

I. INTRODUCTION

The dc power transmission and distribution have been extensively adopted due to their advantages, such as higher efficiency, asynchronous operation, and high flexibility. DC power network finds various applications, including renewable energy integration, electrified transportation, which includes aircraft and ships, high-power energy storage systems, and military systems [1], [2]. Radar is a primary civil and

military equipment that helps in detecting and gathering information about aircraft and missiles. The radar generally consists of various subsystems such as radar processing unit, radar operator console, phased array antenna, radar power system (RPS), and cooling system. Long-range radars that can track objects from hundreds of km demand huge electrical power in the order of tens of kW. All the subsystems except the antenna of the radar work on an ac power supply. The phased array antenna of a radar typically houses a large number of electronic components that primarily require dc power and consume almost half the total RPS capacity. Military systems need to have the highest operational reliability, and all the subsystems need to meet the requirements individually. Long-range radars demand significant electrical power in the form of dc, and the protection of such a system becomes the utmost priority. On these lines, the development of DCCBs for radar applications gained significant interest. The main components of a radar antenna that house critical electronics are the exciter receiver unit, antenna array electronics units, aray controller units, and transmit/receive modules (TRM). These units get dc power from the rectifier system through circuit breakers (CB) which are based on mechanical switches at present and are very slow. The dc power system used in radar power distribution is not very different from the low voltage dc (LVdc) grids, and the protection schemes developed for LVdc grids can directly fit into radar applications, by meeting additional military qualification standards.

Recently, LVdc systems gained a lot of importance due to their easy integration with local energy sources and ease of control. The absence of zero current crossing in the dc system current makes it very difficult to interrupt the short-circuit and over-current faults. Researchers in academia and industry have been extensively studying this topic and presented several DCCBs [3], [4], [5], [6]. DCCBs in the literature are broadly classified as MMCBs, SSCBs, and HCBs [1], [2], [7]. The MMCBs adopt *LC* resonant circuits to create artificial current zero crossings that further help in faster arc quenching between the mechanical switch contacts. The MMCBs are considered in applications where there are no critical loads and sources, as the total fault interruption speed of MMCBs ranges from 50–100 ms, making them a less reliable option. Additionally, the passive components result in an oversized system. The SSCBs, on the other hand, replace the conventional mechanical switch with a semiconductor device or a combination of them. The SSCBs, as the name suggests, are semiconductor-based switches and aid in interrupting a short circuit fault within a few microseconds. However, SSCBs contribute significant conduction power losses and further demand for an extra cooling system [8], [9]. Recent advancements in semiconductor devices made extra efforts to reduce the conduction power losses [10], however, the short-circuit current withstanding capability still needs improvement, as the dc grid results in severe fault currents due to negligible impedance.

The HCB uses solid-state devices (such as MOSFET, IGBT, IGCT, etc.) and ultrafast mechanical switches (MCBs). The HCB presents remarkably lower conduction power losses, similar to the MCBs used in ac power systems. Additionally, the fault interruption speed of the HCB is also better compared to the MMCBs [7], [11], [12], [13], [14], [15]. However, the fault interruption speed of almost all the existing HCBs depends completely on the speed (turn-ON delay plus the reaction delay) of the mechanical switch or the disconnector. The authors in [16], [17], and [18] presented a new family of HCBs that provide ZCS and/or ZVS features. However, most of these topologies employ a precharged capacitor and precharging circuits—to create a zero current or zero voltage condition in/across the mechanical switch.

Following is the summary of the features of the existing HCB configurations (though there is extensive literature), this article considers only the most relevant literature.

1) The HCB topologies presented by [11], [12], and [13] use PEM that are developed by using semiconductor devices. The PEMs are connected in parallel to the MCB, and the current commutation takes place through the fault/load. This forces the PEM to conduct for a longer duration until the mechanical switch contact separates and gains its dielectric capabilities.
2) Load-side fault interruption depends on the speed of the mechanical switch's dielectric recovery capability. This makes all the components that form the current path for fault carry the fault current for a longer time and leads to overstress.
3) The existing HCB topologies largely employ precharged capacitors and their corresponding precharging circuits for creating ZCS/ZVS features.
4) Current transfer from the MCB to the semiconductor branch takes place only after the separation of the mechanical switch contacts, except in [11], etc.
5) Few HCB topologies, including [11] and [18] use series connected power electronic devices, resulting in extra power losses. Further, these topologies demand parallel connections of power devices for high-current applications. The main advantage of this configuration is that it provides ultrafast fault current interruption, but requires an ultrafast mechanical switch to support the system voltage-blocking capability (as this class of HCB uses low voltage-rated power semiconductor devices).
6) The mechanical switch/contact operates reliably and the life cycle is of the order 10 000. However, the life cycle can be significantly improved to 100 000 if the contact is opened at ZVS and ZCS conditions [DCNEV250-MA].

Therefore, this article proposes a ZVS and ZCS-based bidirectional hybrid dc circuit breaker (ZVS-ZCS-HCB) topology incorporating PEMs connected in parallel to the dc source and a series current limiting inductor combination. The proposed ZVS-ZCS-HCB can be easily adapted for various applications involving low voltage dc. The proposed CB would be an excellent addition to future radars including electrified aircraft and ships. The proposed topology connects the PEMs between the positive and negative rails of the dc system as soon as the fault is detected. Following are the main

features of the proposal: 1) zero current switching opening of MCB; 2) zero voltage switching opening of the MCB; 3) no need of capacitors for accommodating ZVS/ZCS features in MCB (IGBT's snubber capacitors are different from these capacitors); and 4) ultrafast load side protection and does not depend on the reaction time of the mechanical disconnector or the MCB. The main advantages of the proposed hybrid dc circuit breaker topology over the existing HCB are ultrafast load side fault interruption, lower conduction losses, simple system, and low cost. Operation of the proposed configuration is validated using LTspice simulations along with an experimental laboratory-scale prototype at a rating of 310 V–10 A, interrupting the dc system fault completely in 4 ms.

The rest of this article is organized as follows. Section II presents the principle of operation of the proposed dc circuit breaker topologies for radar dc power distribution applications. A detailed discussion of component selection is presented in Section III and the software implementation is discussed in Section IV. Experimental prototype and hardware implementation are elaborated in Section V. A discussion on the performance comparison and limitation of the proposed circuit breaker is elucidated in Section VI. Finally, Section VII concludes this article.

A. ABBREVIATIONS AND ACRONYMS

CB	Circuit breaker.
DCCB	DC circuit breaker.
HCB	Hybrid circuit breaker.
LVdc	Low voltage dc.
MCB	Mechanical circuit breaker.
MMCB	Modified mechanical circuit breaker.
MOV	Metal oxide varistor.
PEM	Power electronic module.
SSCB	Solid state circuit breaker.
ZCS	Zero current switching.
ZVS	Zero voltage switching.
i_{MCB}	MCB current.
v_{MCB}	Voltage across MCB.
i_{Q1a}	PEM modules Q_{1a} device current.
i_{Q2a}	PEM modules Q_{2a} device current.
i_{Q1b}	PEM modules Q_{1b} diode current.
$i_{L_{ga}}$	Input grid side inductor current.

II. OPERATING PRINCIPLE OF THE ZVS-ZCS-HCB

Preliminary CB topology with unidirectional operation has been discussed in [19]. The circuit schematic of the proposed ZVS-ZCS bidirectional hybrid dc CB is elucidated in Fig. 1. In the ZVS-ZCS-HCB, a mechanical contactor (MCB), two current limiting inductors—one on each port (L_{ga} & L_{gb}), two PEMs (Modules A & B), and two sets of damping resistors and diodes (D_a & D_b, R_{da} & R_{db}) are used. Each PEM consists of IGBTs, current limiting resistors, and MOVs as shown in Fig. 1. The proposed dc circuit breaker has two ports capable of protecting a dc system in both directions. Hence, the voltage source and loads can be connected accordingly.

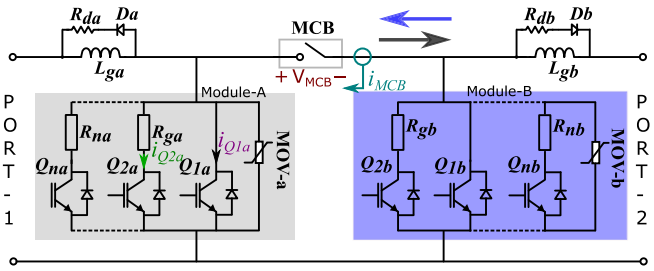

FIGURE 1. Schematic of the proposed ZVS-ZCS-HCB topology.

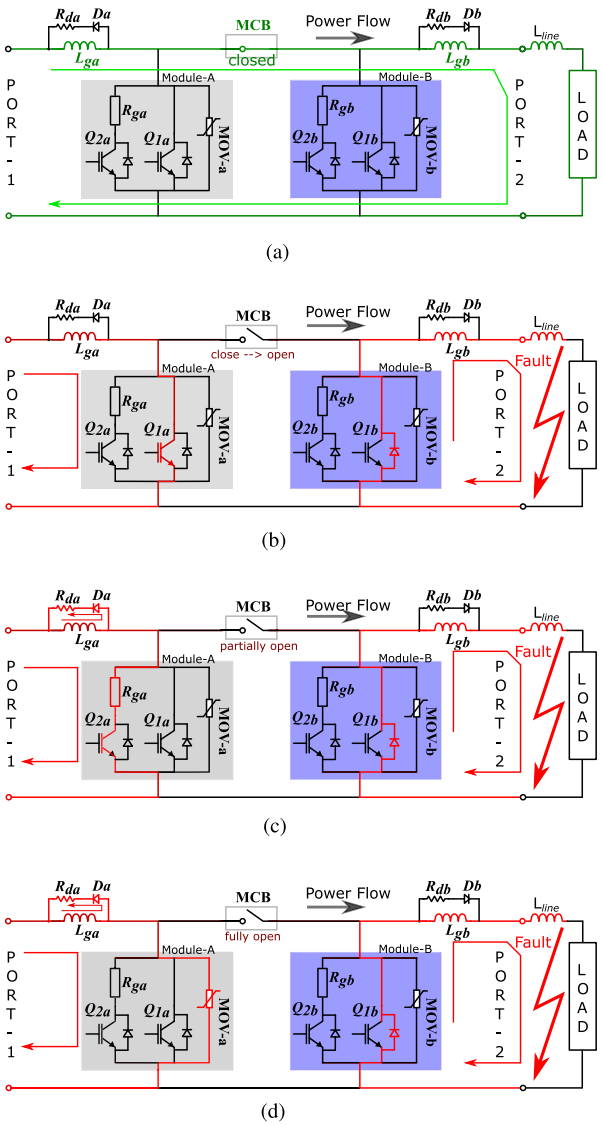

FIGURE 2. Modes of operation of the proposed ZVS-ZCS-HCB topology. SC fault: Short-circuit fault.

The gray shaded circuits are for forward power flow from PORT-1 to PORT-2, while the blue shaded circuit corresponds to reverse power flow from PORT-2 to PORT-1. The parameter L_{line} shown in Fig. 2 represents transmission line inductance. Transmission line resistance is avoided for convenience. With more parallel branches (Q_{na} and Q_{nb}) in the PEM modules

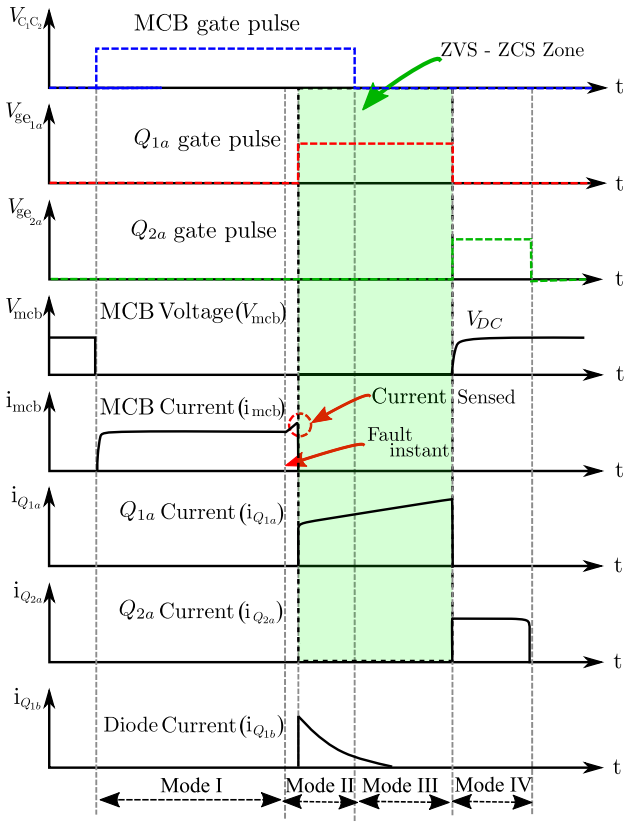

FIGURE 3. Conceptual waveform depicting various instants of the proposed ZVS-ZCS HCB.

(Modules A and B), more steps (staircase waveform) in the input current are achieved, leading to reduced voltage stress across the MCB during the contact opening. The complete working principle of the proposed CB is elucidated in Fig. 2. The control and gate pulse timing diagram is elucidated in Fig. 3. As the circuit is symmetric, only power flow from PORT-1 to PORT-2 is discussed. The green and red color solid lines show the current path during normal and fault interruption operations, respectively.

1) Mode-I: During this mode, power flows from the source to the load through MCB, as shown in Fig. 2(a). All the devices of Module-A and Module-B are kept in OFF-state.
2) Mode-II: A fault is emulated by shorting the load terminals on PORT-2 (solid red line), as shown in Fig. 2(b). The MCB current is continuously monitored using hall effect current sensors and fed to the controller, which compares with the preset fault value and issues a gate command for the IGBTs. As soon as the fault current crosses the set value, a command to turn ON IGBT Q_{1a} and a command to turn-OFF MCB is given. As a result, the entire MCB current transfers to IGBT Q_{1a}. Further, it creates a zero current crossing in the MCB. Simultaneously, the energy stored in the line inductor (L_{line}) and current limiting inductor (L_{gb}) forces the antiparallel diode of IGBT (Q_{1b}) into conduction. As a result, two terminals of the MCB are clamped to near-ground potential and create a ZVS condition. Though the MCB is given a turn-OFF command as soon as the fault is detected, it takes a much longer time to respond and start to open its contacts (delay + response time). As the MCB experiences both ZCS and ZVS conditions, it results in an arcless fault interruption. This stage isolates the load-side systems and ensures their protection.
3) Mode-III: In the previous mode, MCB is issued a turn-OFF signal, but its contacts take a significant amount of time to separate due to the turn-OFF delay and mechanical inertia (around 3.7 ms for the dc contactor used in the present prototype). Once the contacts separate by a minimum distance, then a turn-ON command to IGBT Q_{2a} is released. Simultaneously, a command to turn OFF Q_{1a} is given. This results in the current transfer from IGBT Q_{1a}–Q_{2a}, as elucidated in Fig. 2(c). The large resistance R_{ga} connected in series with Q_{2a} limits the current drawn from the source, and hence Q_{2a} could then be turned OFF at a minimum current condition. The initial stored energy in L_{ga} partially damped out using a damping circuit as shown in Fig. 2(c). A number of stages in the PEM modules could be created for smooth current transfer, and create a staircase waveshape in the input current. The transmission line inductance takes the path discussed in the previous mode until the inductive energy is fully damped or recovered.
4) Mode-IV: Once the MCB is fully open, a turn-OFF signal to IGBT Q_{2a} is given. As a result, the energy stored in the inductor L_{ga} and extra stray inductances of the grid side is recovered by MOV and damping circuit as shown in Fig. 2(d). This finally results in a complete fault interruption without any arc in the MCB.

During Mode-II through Mode-IV, the energy stored in load side inductors (L_{gb} and L_{line}) forces the antiparallel diode of the IGBT Q_{1b}, which provides a freewheeling path for the current. The energy in these inductors dissipates in series resistors (equivalent series resistance of inductors), fault resistance, and diode (due to forward voltage drop). Once the inductors demagnetize completely, current flowing through the diode (Q_{1b}) dies down to zero, as depicted in Fig. 3. The proposed DCCB gives designers greater flexibility in setting the system parameters according to the requirements, such as 1) over-current/short-circuit protection setting; 2) multiple modules for modularity; 3) maximum fault current; and 4) the reclosing time.

III. COMPONENTS SELECTION AND DESIGN

This section presents the guidelines for component selection (IGBTs, MCB, inductors, and resistors). This section also highlights constraints related to MCB and limitations on designing the inductor L_{ga}, and these factors limit testing of the CB. The MCB tripping time is the major limitation on which the turn-ON duration of the IGBT Q_{1a} and inductance value rely. There are two different MCBs (LEV100A5ANG - 18 ms and DCNEV250-MA - 3.8 ms) used for the experiment to

TABLE 1 Hardware Parameters and Component Details

Components	Description
Input Voltage (DC)	310 V DC (enArka 400 V/25 A power supply)
Input current	10 A rated and 15 A fault current
Power (in kW)	3.1 kW (rated), and 4.65 kW (during the fault)
MCB	LEV100A5ANG (900V/100A) -TE Connectivity
MCB	DCNEV250-MA (900V/250A) -Littelfuse
Q_{1a}& Q_{2a}	SKM150GB12T4 (1200V/150A) -Semikron
L_{ga}	29 mH (Custom made)
R_{ga}	40 Ω
R_{da}	5 Ω
Microcontroller	MSP430FR2355 (Texas Instruments)

study the importance of contactor open time at zero current which is listed in Table 1. MCB (DCNEV250-MA) with approximately 3.8 ms open time with zero current is used in the experiment setup. To avoid restriking of MCB and to ensure the reliable ZVS and ZCS operation of the proposed CB, the turn-ON duration of the IGBT Q_{1a} (ΔT_{ON}) must be greater than or equal to the tripping time of the MCB as given in the following:

$$\Delta T_{\text{ON}} \geq 3.8\, ms. \tag{1}$$

Since the line inductance is very low, an external inductor L_{ga} is introduced to limit the short circuit current resulting from the IGBT Q_{1a} turn-ON. The nominal load current of the proposed CB considered for validation is 10 A. Assuming the change in current magnitude through IGBT Q_{1a} during ΔT_{ON} to be four times the nominal current and ΔT_{on} as 3.8 ms, the value of L_{ga} can be calculated by the following:

$$L_{ga} = V\,\frac{\Delta T_{\text{ON}}}{\Delta I_L} \tag{2}$$

L_{ga} is the desired value for a system with a voltage of 310 V dc to exhibit a linear current profile during ΔT_{ON}. From (2) L_{ga} is found as 29.45 mH. The inductance value is highly dependent on the response time of the mechanical switch, a faster MCB would significantly reduce L_{ga} value to as low as few μH. For example, an ultrafast disconnector can open the contacts in less than a millisecond, hence would require a very small value of inductance.

A. SELECTION OF IGBTS Q_{1a} AND Q_{2a}

The required dc blocking voltage of IGBTs Q_{1a} and Q_{2a} in the OFF-state condition is around 310 V. The peak current through the IGBT Q_{1a} is limited by the L_{ga} and ΔT_{ON} selections. According to the aforementioned calculations, the maximum current that Q_{1a} required to carry is 40 A. The voltage induced across the IGBT during the turn-OFF transient of Q_{1a} is typically the sum of dc bus voltage and the voltage spike caused by the inductor L_{ga}. The total voltage peak is approximately twice the steady-state dc voltage. This voltage should not be higher than the IGBT's peak voltage capability. A resistor that is added in series with the IGBT Q_{2a} further decreases the

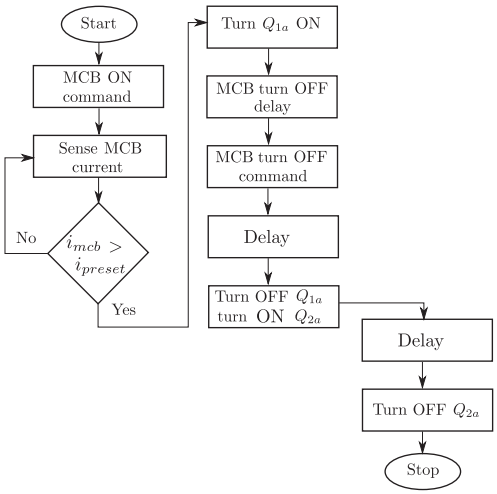

FIGURE 4. Control flowchart for the proposed ZVS-ZCS HCB.

current flowing through the system. Taking the above aspects into consideration, an IGBT power module from Semikron has been used for the CB prototype and validation. Table 1 presents the list of components selected for the prototype.

IV. SIMULATION VALIDATION

The proposed DCCB has been simulated in the LTspice software environement, which provides PSpice based simulation capabilities, and its operation is validated for various operating conditions. The operation and control implementation used for the proposed CB is shown in Fig. 4. The MCB is emulated by using the semiconductor switches by adding an extra high-value capacitor across the gate-source terminal. Challenges associated with the inductor design, especially for the proposed circuit and the associated effect on the fault interruption performance, have been verified. For the present simulation study, a 310 V dc with a rated current of 10 A and a fault current preset limit of 15 A is considered to highlight the sensitivity capabilities. Fig. 5 shows the simulation waveforms of various components during all the modes, i.e., during starting, steady-state operation, faulty mode, and fault interruption. The dc system is energized at 1 ms, which takes about 6 ms to reach steady-state operation. At 8 ms, a fault is created by shorting the output terminals; as a result, the system current increases slowly due to the presence of inductors. As soon as the current reaches 150% of the rated current (at 10 ms), the controller issues a command to turn ON Q_{1a} and turn OFF MCB simultaneously. As the impedance offered by the Q_{1a} branch is lower compared to the load side fault branch, MCB current (i_{mcb}) instantly transfers to Q_{1a} and creates a zero current in the MCB. As the Q_{1a} connected in parallel to the dc source, provides a ZVS characteristic for MCB as both terminals of the MCB are pulled down to zero during this time interval. As MCB takes more time to respond, hence this time interval is kept high and can be reduced if there is an ultrafast mechanical contactor. After a few milliseconds, a command to turn ON Q_{2a} and turn OFF Q_{1a} is released, as a result,

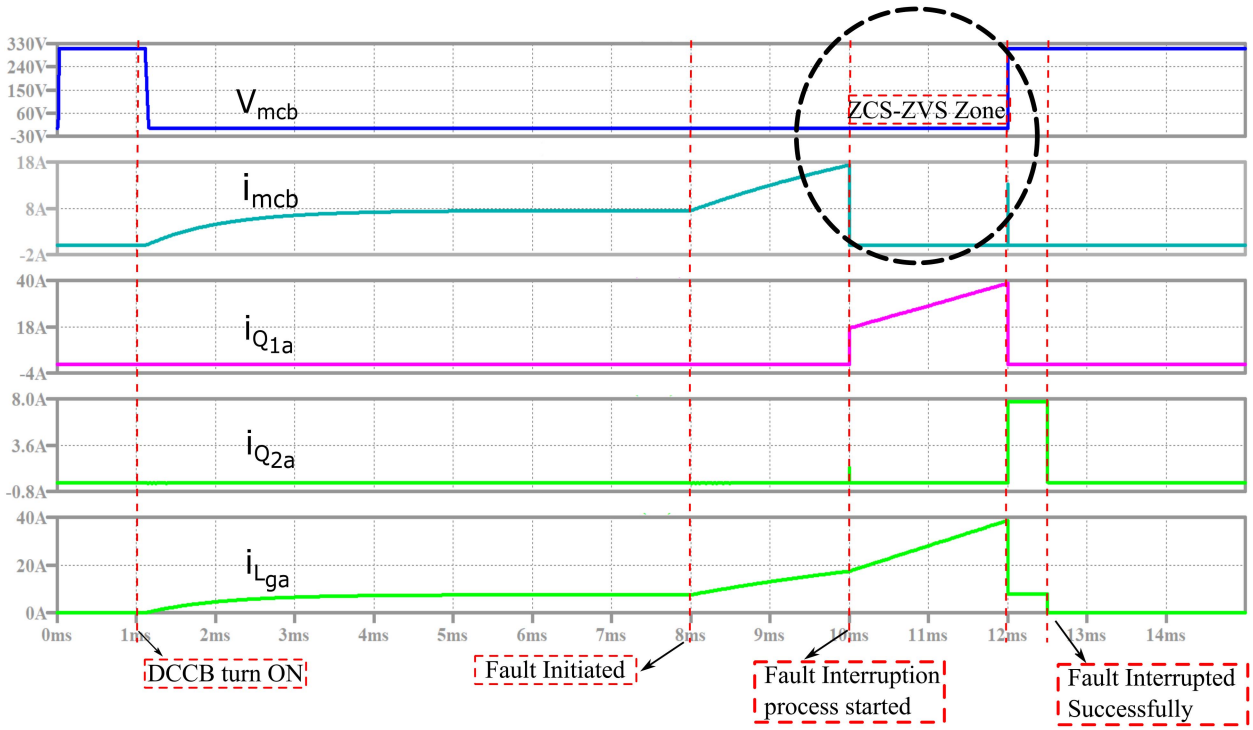

FIGURE 5. Simulation results of the proposed DCCB showing various modes of operation—starting, steady-state operation, fault, and fault interruption.

the current transfer takes place from Q_{1a} to Q_{2a} as given in Fig. 5. As a series resistance exists with Q_{2a}, the total input current reduces, and the input current will have a staircase step-down waveform, which is elucidated in Fig. 5. During the entire fault interruption process, it may be noted that the MCB experiences both ZVS and ZCS characteristics, resulting in arcless and faster MCB operation, which is an important feature of the proposed HCB. An experimental proof that agrees with the simulation results is elucidated in the following sections.

V. EXPERIMENTAL VALIDATION

A. EXPERIMENTAL SETUP OF THE PROPOSED HCB

The proposed ZVS-ZCS-HCB topology is validated experimentally for a 310 V–10 A dc system. The MCB is emulated using dc contactor (DCNEV250-MA) of make from Littelfuse with a 900 V–250 A rating. The selected MCB (dc contactor) has a turn-OFF delay of 3.8 ms. Semikron provides the IGBTs SKM150GB12T4, having 1200 V–150 A, which are used for devices Q_{1a} and Q_{2a}.

The inductor (L_{ga}) is selected as 29 mH (custom-made in the laboratory), R_{ga} of 40 Ω is connected in series with Q_{2a}. A LEM LA55-P current transducers and the MSP430 microcontroller form the sense and control circuitry. An enArka make 400 V–25 A (40 A transient current) dc supply is used as a dc power source. The complete list of components used to develop the prototype is summarized in Table 1. The schematic of the experimental configuration is elucidated in Fig. 6. A photograph of the corresponding experimental hardware setup is presented in Fig. 7.

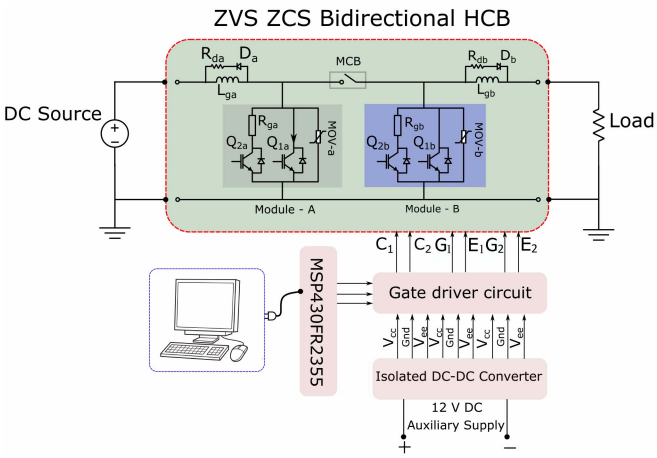

FIGURE 6. Schematic of the testing configuration.

B. EXPERIMENTAL RESULTS AND DISCUSSION

PORT-1 of Fig. 1 is connected to the 310 V dc source, PORT-2 is connected to the load bank. Under normal operating conditions, with MCB in on state, a steady-state current of 10 A flows from PORT-1 to PORT-2 as shown in Fig. 2. A faulty situation is created at time interval t_1 by shorting the terminals of PORT-2. As a result, the current drawn from the source increases linearly from 10 to 15 A. After sensing the overload fault of 15 A, 500 μs of sensing and control delay approximately considered, a turn-ON signal for Q_{1a} and turn-OFF signal to MCB is issued at an instant t_2. As a result, the MCB current transfers immediately to Q_{1a} and is limited to 25 A

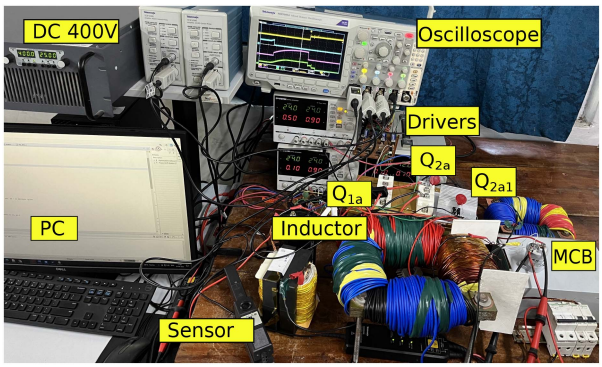

FIGURE 7. Experimental setup, 310 V/10 A, MCB with 3.8 ms opening, fault current of 15 A.

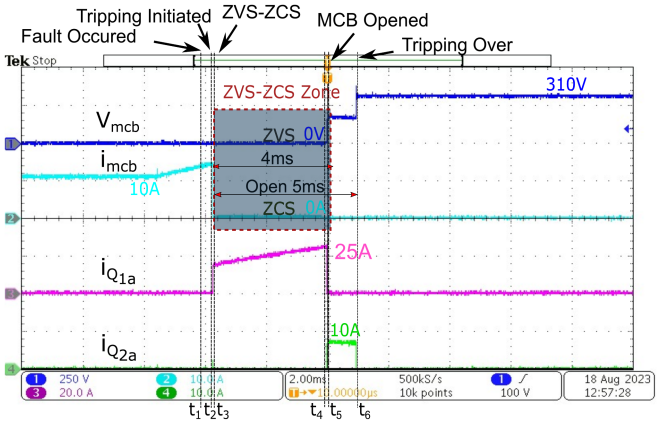

FIGURE 8. DC fault current 15 A interruption results of ZCS-ZVS-HCB - Current transfer. t_1 – *Fault*, t_2 – Q_{1a} ON, t_3–MCB open starts, t_4–MCB opened, t_5 - Q_{2a} ON, Q_{1a} OFF, and t_6 – Q_{2a} OFF - extra delayed.

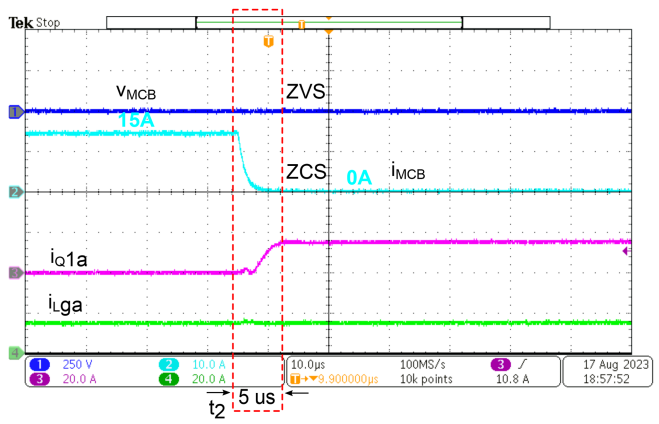

FIGURE 9. Experimental results showing current transfer from MCB to IGBT Q_{1a} in less than 5 μs, and faster load-side fault interruption.

by dc source at 310 V dc; the corresponding result is shown in Fig. 8. The zoomed waveform showing the ultrafast current transfer from MCB to Q_{1a} is elucidated in Fig. 9. The selected MCB has an inherent turn-OFF delay of 3.8 ms; hence Q_{1a} in the present configuration is made to conduct for 4 ms. During this interval, as highlighted in Fig. 8, the voltage across and current flowing through the MCB is observed to be zero. This

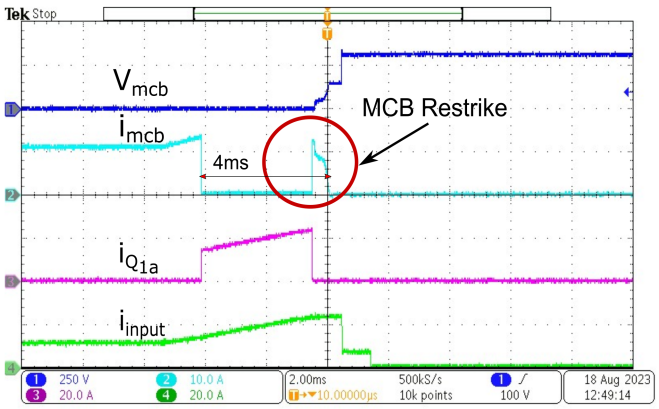

FIGURE 10. Experimental results with 4 ms MCB showing restriking process due to reduction in the turn-ON duration of Q_{1a} to 3.5 ms.

results in an arcless fault interruption. At t_4 that is, after 4 ms delay, MCB is completely opened. At time interval t_5, IGBT Q_{2a} is turned ON and simultaneously Q_{1a} is turned-OFF, that further helps in transferring current from Q_{1a} to Q_{2a}. It can be seen in Fig. 8 with resistance R_{ga} current flow through line inductor is controlled.

From the above experimental results, as elucidated in Figs. 8 and 9, it may be noted that the load-side fault current reaches zero in a few microseconds, and load-side sensitive systems are protected very quickly as soon as the fault is detected. However, the total fault interruption time depends only on the MCB reaction time, which is approximately 4 ms in the present prototype. An ultrafast switch can help in lowering the value of the current limiting inductor for a given system.

To understand the effect of MCB reaction time on the fault interruption process, a short turn-ON duration of 3.5 ms is provided to IGBT Q_{1a}. The corresponding results are elucidated in Fig. 10. The MCB undergoes restriking as its contacts have not fully opened, and voltage blocking capability is not restored. Therefore, the time duration for the overall fault interruption process is fully controlled by MCB reaction time. However, the load-side equipment is protected independent of MCB open time, as the load-side current is pulled to zero as soon as the fault is detected in just less than 5 μs. This is one of the important and positive factors of the proposed configuration.

The experimental prototype is tested with two branches within the PEM module, with devices Q_{1a} and Q_{2a}. As a result, the input current experiences a staircase waveform—down steps, as shown in Fig. 11. The resistance (R_{ga}) connected in series with Q_{2a} reduces the input current and helps limit the input current during the fault interruption process. The fault interruption time is optimized to approximately 4 ms, which does not create restriking in MCB. As discussed in Section II, the energy stored in load side inductors (L_{gb} and L_{line}) forces the antiparallel diode of the IGBT Q_{1b}, which provides a freewheeling path for the current. The energy in these inductors dissipates in series resistors (equivalent series resistance of inductors), fault resistance, and diode (due

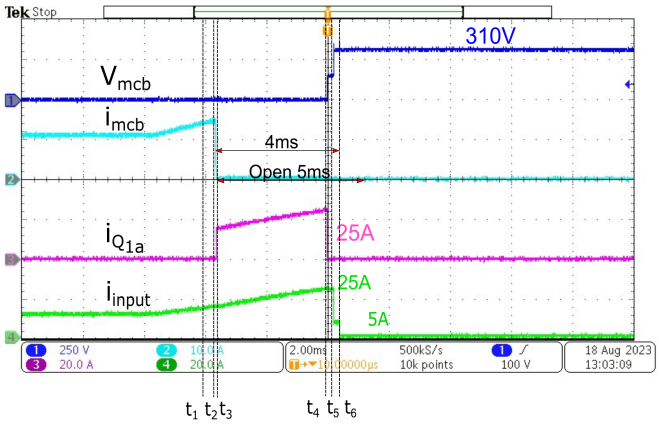

FIGURE 11. DC fault current 15 A interruption results of ZCS-ZVS-HCB of 4 ms MCB opening with two parallel branches Q_{1a} and Q_{2a}.

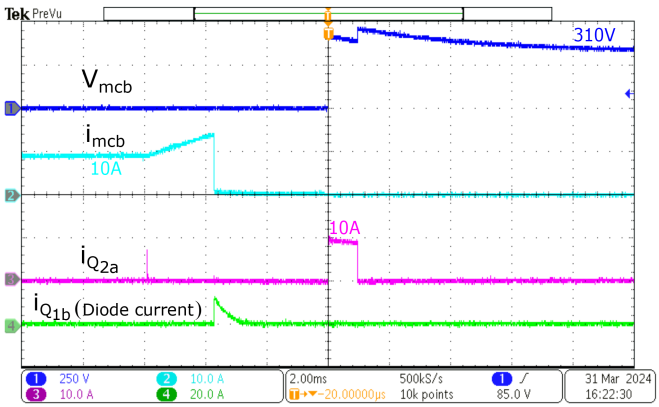

FIGURE 12. DC fault current 15 A interruption results of ZCS-ZVS-HCB showing Q_{1b} diode current.

to forward voltage drop). Once the inductors demagnetize completely, the current flowing through the diode (Q_{1b}) dies down to zero in less than a millisecond; the same is justified using experimental results as presented in Fig. 12. Multiple stages can be added to further reduce the current stress on PEMs and also help in developing systems for high-current applications. The second-biggest advantage of the proposed topology is that the MCB experiences ZCS and ZVS features, which significantly improves the life cycle of the MCB from 10 000 cycles to 100 000 cycles (the maximum life cycle of the MCB).

VI. COMPARISON AND DISCUSSION

Performance of the proposed DCCB topology with the already existing HCB topologies reported in literature [13], [14], [15], [16], [21], [22], [23], and [7] for LVdc application is discussed and a summary highlighting various performance indices is elucidated in Table 2. Though the CB topology reported in [7], has the current limiting capability, the ZCS and ZVS features are not possible. Also, the auxiliary circuit requirement is complex with a pulse transformer. The proposed topology uses PEMs to bypass the fault current and isolate the load from the fault current, which meets the essential requirement of the CB in isolating the load from the fault. Whereas the existing topologies (topologies reported in the literature) allow the fault current to continue to flow through the load till the complete fault interruption process is complete. Therefore, the load experiences large fault currents, and the critical load may be damaged.

1) The HCB topologies presented by [12] are essentially developed for HVdc application. These HCBs use PEM, capacitors, and inductors that are connected in parallel to the mechanical switch. The current commutation takes place through the fault/load. However, in the proposed topology, the PEM bypasses the fault current path, and the fault current flowing through MCB is instantaneously pulled to zero. This further creates a ZCS and ZVS feature, providing an arcless fault interruption. From the earlier discussion, it may be noted that the proposed HCB does not use any precharged capacitor to achieve the ZCS and ZVS features.
2) The load side instantaneously gets isolated (current becomes zero) in the proposed topology in less than 5 μs, resulting in a very fast load-side protection. The same is not the case with the existing HCB topologies.
3) HCB [13], [14], and [16] have a similar limitation of allowing the fault current to flow through the load till the fault is completely interrupted.
4) HCB [13], [14], and [16] have to use PEM to cater for supplying fault current during the interruption process. PEMs used in the abovementioned HCB are developed using IGBTs, hence, the device peak current rating has to cater to fault current. In the proposed HCB, as the current is limited by the internal line inductor and internal resistance of the source, the peak current requirement of the device can be optimized.
5) Topologies presented in [14] and [16] have the fault current limiting capability due to series inductor, however, ZCS operation of the main MCB is not possible.
6) With the comparable number of PEM (switches), inductors, and capacitors, the bidirectional capability of the proposed HCB is a merit. Though the CB topology reported in [7], has the current limiting capability, the ZCS and ZVS features are not possible. Also, the auxiliary circuit requirement is complex with a pulse transformer. Additionally, the opening time is determined by the opening time of MCB. As ZCS is not possible, the MCB contacts experience arcing, which further leads to reduced operational cycles.
7) The DCCB topologies reported in [21], [22], and [23] have been compared with the proposed topology and summarized in Table 2. The performance of the proposed topology is on par with the reported topologies.

The main features of the proposed topology are: 1) zero current switching opening of MCB; ii) zero voltage switching opening of the MCB; 3) no need of capacitors for accommodating ZVS/ZCS features in MCB (IGBT's snubber capacitors

TABLE 2 Performance Comparison of Various HCB Topologies for LVDC Application

Parameters	[6]	[13]	[14]	[15]	[16]	[7]	[20]	[21]	[22]	[23]	ZCS-ZVS HCB
Instant isolation of load from fault current	Yes	No	No	No	Yes	No	No	No	No	No	Yes
Tripping time at Fault current at System voltage	2.4 μs 170 A 375 V	23 ms 20 A 300 V	3.3 ms 80 A 200 V	4 ms 1200 A 500 V	3 ms 20 A 300 V	3.5 ms 30 A 600 V	2 ms Sim 1000 V	2 ms Sim 1000 V	600 μs 148 A 600 V	7.5 ms Sim 400 V	4 ms 20 A 310 V
Fault current limiting capability	Yes	No	Yes	No	Yes	Yes	No	Yes	No	Yes	Yes
ZCS of main CB / Contactor	Yes	Yes	Yes	Yes	Yes	No	N/A	N/A	Yes	Yes	Yes
ZVS of main CB / Contactor	No	No	No	No	No	No	N/A	N/A	No	No	Yes
Number of switches (IGBTs, CBs, Contactors, SCRs)	3	6	3	5	3	4	8	4	11	6	7
Number of inductors	0	0	2	1	2	3	2	3	1	2	2
Number of capacitors	1	1	2	1	1	2	1	1	2	3	0
Bidirectional capability	No	No	No	No	No	No	Yes	Yes	Yes	Yes	Yes
Fault current commutation through load	No	Yes	Yes	No	Yes	No	Yes	Yes	Yes	Yes	No
Fault current flow through PEMs	No	Yes	Yes	No	Yes	No	Yes	Yes	Yes	Yes	Yes$^{\$}$

Note: Sim: Simulations; $ - fault current flows through PEMs in the receiving end only for a couple of μS.

are different from these capacitors); and 4) the ultrafast load side protection is achieved in less than 5 μs for 15 A fault current, which does not depend on the reaction time of the mechanical disconnector or the MCB. The life span of the MCB greatly depends on contact arcing. As the proposed topology exhibits ZVS and ZCS features, arcless operation is possible, and as a result, the life span of the MCB is significantly improved.

Though the proposed topology exhibits several merits, the overall fault interruption is largely limited by the MCB reaction. MCB reaction time also brings several challenges while designing the current limiting inductor, especially for high-power dc systems. In the present experimentation, an inductor of 29 *mH* is used as the MCB takes about 3.8 ms to open and close its contacts. From the data-sheet of the contactor DCNEV250-MA, the estimated life cycle of 10 000 cycles make/break at a rated current of 250 A is increased to more than 100 000 cycles at zero current. Hence, the reliability of dc protection significantly improved with the proposed topology configuration, as the mechanical contact reliability improved, which is close to the reliability of PEMs. Higher reliability is the most important requirement for dc power distribution in RPSs. The proposed topology will be an excellent option if MCBs with better fault interruption speeds of the order 1–2 ms (Thomson coil-based ultrafast disconnectors) are available and used.

Compared with other similar bi-directional HCBs, the proposed HCB offers several advantages. Notably, it has a lower component count, consisting of only nine components, including switches and inductors. Additionally, there is no need for a capacitor for commutation purposes. The tripping time after a fault is comparable to that of other HCBs within the same range, primarily limited by the opening time of the MCB. The main benefit of the proposed ZCS-ZVS DCCB is that it contributes to the improved reliability of the proposed HCB. Furthermore, fault current commutation through the load occurs for a shorter duration, proportional to the load-side inductance due to the free-wheeling diode of Q_{1b}. Unlike other HCBs where the source supplies fault current and flows through the load, the proposed HCB minimizes the magnitude of fault current flowing through the load, which is less than a millisecond.

VII. CONCLUSION

This article presents a hybrid DCCB topology that results in ZVS and ZCS features and further provides an arcless fault interruption. The proposed topology is analyzed and simulated using the LTspice platform. Later, a lab-scale prototype of 310 V–10 A (25 A fault current) is developed to experimentally validate the performance. The proposed topology successfully isolates the load section from the fault in just less than 5 μs and it takes about 4 ms for the complete opening of the MCB. The arcless interruption process in the proposed HCB importantly helps in improving the life span of the MCB as well as the reliability of dc power protection in the RPS.

REFERENCES

[1] C. M. Franck, "HVDC circuit breakers: A review identifying future research needs," *IEEE Trans. Power Del.*, vol. 26, no. 2, pp. 998–1007, Apr. 2011.

[2] A. Shukla and G. D. Demetriades, "A survey on hybrid circuit-breaker topologies," *IEEE Trans. Power Del.*, vol. 30, no. 2, pp. 627–641, Apr. 2015.

[3] R. Rodrigues, Y. Du, A. Antoniazzi, and P. Cairoli, "A review of solid-state circuit breakers," *IEEE Trans. Power Electron.*, vol. 36, no. 1, pp. 364–377, Jan. 2021.

[4] T. Li, Y. Li, and N. Liu, "A new topological structure of Z-source DC circuit breaker," *IEEE Trans. Circuits Syst. II: Exp. Briefs*, vol. 69, no. 7, pp. 3294–3298, Jul. 2022.

[5] V. R. I, S. N. Banavath, and S. Thamballa, "Modified Z-source DC circuit breaker with enhanced performance during commissioning and reclosing," *IEEE Trans. Power Electron.*, vol. 37, no. 1, pp. 910–919, Jan. 2022.

[6] R. Kheirollahi, S. Zhao, and F. Lu, "Fault current bypass-based LVDC solid-state circuit breakers," *IEEE Trans. Power Electron.*, vol. 37, no. 1, pp. 7–13, Jan. 2022.

[7] Z. J. Shen, Y. Zhou, R. Na, T. Cooper, M. A. Ashi, and T. Wong, "A series-type hybrid circuit breaker concept for ultrafast DC fault protection," *IEEE Trans. Power Electron.*, vol. 37, no. 6, pp. 6275–6279, Jun. 2022.

[8] V. Raghavendra I, B. S. Naik, T. Sreekanth, and A. Chub, "Controlled bidirectional DC circuit breaker with zero negative current for high load shift applications," *IEEE Trans. Ind. Appl.*, vol. 58, no. 6, pp. 6942–6951, Nov./Dec. 2022.

[9] J.-Y. Yu, J.-Y. Kim, S.-M. Song, Z. Ayubu, and I.-D. Kim, "New DC solid-state circuit breaker with natural charging operation," *IEEE Trans. Ind. Electron.*, vol. 68, no. 11, pp. 10360–10368, Nov. 2021.

[10] N. Boettcher and T. Erlbacher, "A monolithically integrated SiC circuit breaker," *IEEE Electron Device Lett.*, vol. 42, no. 10, pp. 1516–1519, Oct. 2021.

[11] M. Callavik, A. Blomberg, J. Häfner, and B. Jacobson, "The hybrid HVDC breaker an innovation breakthrough enabling reliable HVDC grids," ABB Grid Systems, Technical Paper, Vasteras, Sweden, Nov. 2012. Accessed: May 16, 2024. [Online]. Available: https://library.e.abb.com/public/c9d5ba256e7e9671c1257ab6004b1feb/hybrid-hvdc-breaker-an-innovation-breakthrough-for-reliable-hvdc-gridsnov2012.pdf

[12] J. Xu, X. Zhao, N. Han, J. Liang, and C. Zhao, "A thyristor-based DC fault current limiter with inductor inserting–bypassing capability," *IEEE Trans. Emerg. Sel. Topics Power Electron.*, vol. 7, no. 3, pp. 1748–1757, Sep. 2019.

[13] C. N. M. Ajmal, I. V. Raghavendra, S. Naik, A. Ray, and H. S. Krishnamoorthy, "A modified hybrid DC circuit breaker with reduced arc for low voltage dc grids," *IEEE Access*, vol. 9, pp. 132267–132277, 2021.

[14] R. Lazzari and L. Piegari, "Design and implementation of LVDC hybrid circuit breaker," *IEEE Trans. Power Electron.*, vol. 34, no. 8, pp. 7369–7380, Aug. 2019.

[15] T. Augustin, M. Becerra, and H.-P. Nee, "Experimental study of enhanced active resonant DC circuit breakers," *IEEE Trans. Power Electron.*, vol. 37, no. 5, pp. 5687–5698, May 2022.

[16] A. Ray, K. Rajashekara, S. N. Banavath, and S. K. Pramanick, "Coupled inductor-based zero current switching hybrid DC circuit breaker topologies," *IEEE Trans. Ind. Appl.*, vol. 55, no. 5, pp. 5360–5370, Sep./Oct. 2019.

[17] S. Teng, Z. Zhang, and L. Xiao, "Research on a novel DC circuit breaker based on artificial current zero-crossing," *IEEE Access*, vol. 8, pp. 36070–36079, 2020.

[18] A. Hassanpoor, J. Hafner, and B. Jacobson, "Proc. technical assessment of load commutation switch in hybrid HVDC breaker," in *Proc. Int. Power Electron. Conf.*, 2014, pp. 3667–3673.

[19] N. Saminathan, C. N. Muhammed Ajmal, S. N. Banavath, and K. Rajashekara, "A zero current switching hybrid circuit breaker for DC grid applications," in *Proc. IEEE Appl. Power Electron. Conf. Expo.*, 2022, pp. 1532–1537.

[20] N. A. W. Song and Y. Wang, "A novel bidirectional t-source DC circuit breaker for DC microgrids," in *Proc. IEEE Conf. Ind. Electron. Appl.*, 2019, pp. 1540–1545.

[21] H. Al-khafaf and J. Asumadu, "Y-source bi-directional DC circuit breaker," in *Proc. Int. Power Electron. Conf.*, Niigata, Japan, 2018, pp. 3445–3449.

[22] N. Shatalov, Y. Zhou, R. Na, and Z. J. Shen, "Design and operation of bi-directional hybrid circuit breaker based on transient commutation current injection," in *Proc. IEEE Appl. Power Electron. Conf. Expo.*, 2021, pp. 1128–1133.

[23] D. Keshavarzi, E. Farjah, and T. Ghanbari, "Hybrid DC circuit breaker and fault current limiter with optional interruption capability," *IEEE Trans. Power Electron.*, vol. 33, no. 3, pp. 2330–2338, Mar. 2018.

NANDAKUMAR SAMINATHAN (Member, IEEE) received the B.E. degree in electrical and electronics engineering from Kongu Engineering College, Bharathiar University, Coimbatore, India, in 1998 and the M.Tech. degree in electronic systems from the Indian Institute of Technology (IIT) Bombay, Mumbai, India, in 2006. He is currently working toward the Ph.D. degree in electrical engineering with the Department of Electrical, Electronics, and Communication Engineering, Indian Institute of Technology Dharwad, Dharwad, India.

He is a Radar Scientist with Electronics and Radar Research Development Establishment (LRDE) under Defence Research and Development Organisation (DRDO), New Delhi, India, for more than 20 years. He has been an External Research Scholar with the Department of Electrical, Electronics and Communication Engineering, Indian Institute of Technology Dharwad, since August 2020. His research interests include antenna power supply, dc power distribution, radar power system, and system engineering.

ADITYA P (Graduate Student Member, IEEE) received the B.Tech. degree in electrical and electronics engineering from Velagapudi Ramakrishna Siddhartha Engineering College, Vijayawada, India, in 2021. He is currently working toward the master's degree in power electronics with the Indian Institute of Technology Dharwad, Dharwad, India.

His current research interests include dc circuit breaker applications in next-gen electric aircrafts and future dc homes, and power converters for electrification transportation.

SATISH NAIK BANAVATH (Senior Member, IEEE) received the B.Tech. degree in electrical and electronics engineering from Acharya Nagarjuna University, Guntur, India, in 2010, the M.E. and Ph.D. degrees in electrical engineering from the Indian Institute of Science, Bengaluru, India, in 2012 and 2018, respectively.

From 2012 to 2014, he was with Defence Research and Development Organization (DRDO), Ministry of Defence, Government of India, Bengaluru, India. He was a Postdoctoral Fellow with the University of Houston, Houston, TX, USA, from 2017 to 2018. Later, he joined Mahindra Electric Mobility Limited where he served as a Research and Development Manager from 2018 to 2019. He is currently working as an Assistant Professor with the Department of Electrical Engineering at the Indian Institute of Technology (IIT) Dharwad, Dharwad, India, where he joined in February 2019. His current research interests include multilevel power converters, power converters for renewable energy conversion, electric vehicles, and dc circuit breakers.

ALESSANDRO LIDOZZI (Member, IEEE) received the electronic engineering and the Ph.D. degree in mechanical and industrial engineering from the Roma Tre University, Rome, Italy, in 2003 and 2007, respectively.

From 2010 to 2017, he was a Researcher with the Department of Engineering, Roma Tre University, where he has been an Associate Professor since 2017. His main research interests include power converter modeling and control, control of permanent magnet motor drives, control aspects for power electronics in diesel–electric generating units, four-leg converters, and the development of high-performance control platforms based on combined DSP-FPGA systems.

Dr. Lidozzi is an Associate Editor for IEEE TRANSACTION ON INDUSTRY APPLICATIONS.

MARCO DI BENEDETTO (Member, IEEE) received the M.Eng. degree in electronic engineering from the University of Roma Tor Vergata, Rome, Italy, in 2014, and the Ph.D. degree in mechanical and industrial engineering from Roma Tre University, Rome, in 2018.

Since 2018, he has been a Research Fellow with the Center of Power Electronics and Drives (C-PED), Roma Ter University. His current research interests include hardware and FPGA control design for multilevel power converter topologies.

A VENGADARAJAN (Senior Member, IEEE) received the B.E. degree in electronics and communication engineering from Madurai Kamaraj University, Madurai, India, in 1985, the M.Tech. degree in microwave engineering and the Ph.D. degree in microwave engineering from the Indian Institute of Technology (IIT) Karagpur, Karagpur, India, in 1992 and 2002, respectively.

He joined DRDO as a Scientist with the Center for Air Borne Studies in 1986. He has worked in various airborne radar projects of DRDO in field of microwave engineering as well as in leadership role as project Director. He is currently working as an Associate Director in Electronics and Radar Development Establishment (LRDE). He has authored or coauthored more than nine publications in international journals in the field of radar. His research interests include signal processing for Doppler radars, SAR, MIMO, and radar system engineering.

Open Access funding provided by 'Università degli Studi Roma Tre' within the CRUI CARE Agreement